A Transformation for Ordering Multispectral Data in Terms of Image Quality with Implications for Noise Removal

ANDREW A. GREEN, MARK BERMAN, PAUL SWITZER, AND MAURICE D. CRAIG

Abstract—**Although principal components transformations on remotely sensed multispectral data often produce components that show decreasing image quality with increasing component number, there are numerous examples, especially among aircraft scanner data, where this is not the case. This has led us to define a new transformation, known as the maximum noise fraction (MNF) transformation, which always produces new components ordered by image quality. It can be shown that this transformation is equivalent to principal components when the noise variance is the same in all bands and that it reduces to a multiple linear regression when noise is in one band only. Noise can be effectively removed from multispectral data by transforming to the MNF space, smoothing or rejecting the most noisy components, and then retransforming to the original space. In this way much more intense smoothing can be applied to the MNF components with high noise and low signal content than could be applied to each band of the original data. The MNF transformation requires knowledge of both the signal and noise covariance matrices. Except when the noise is in one band only, the noise covariance matrix needs to be estimated. One procedure for doing this is discussed and examples of cleaned images are presented.**

I. Introduction

PRINCIPAL components (PC) transformations have become a standard tool for the compression and enhancement of remotely sensed multispectral data (e.g., [1]–[3]). It has been noted [1]–[3] that the high between-band correlation that often exists in multispectral data can lead to a compression of image information into the low-order principal components. This compression is manifested as a steadily decreasing signal-to-noise ratio as the PC number increases. Although this trend is almost always observed with Landsat data, we and others [4] have found a number of cases where airborne thematic mapper (ATM) simulator data do not behave in this way.

Fig. 1 shows the first, fourth, sixth, and ninth principal component images for (ten-band) ATM data collected over the Silver Bell district in Arizona. Although the first few principal components behave much as expected, there is no definite trend to increasing noise with increasing component number. Indeed, the ninth principal component is quite an acceptable image with less noise than the fourth or sixth principal components. In an earlier statistically oriented treatment of this problem [5], Switzer and Green showed how to define a new transformation that ordered images into components of increasing spatial autocorrelation. In the present paper we recast and expand the procedure more directly in terms of signal-to-noise (S/N) ratios, and show how it may be used to improve standard methods of noise removal and image enhancement.

First, we develop the maximum noise fraction (MNF) transform as a method for ordering components in terms of image quality. Two special cases are discussed. The first case shows the relationship between the MNF transform and principal component analysis, and the second treats the situation when noise is found in one band only.

Then we apply the MNF transform to noise removal and discuss how *spatial* information can be used to estimate the covariance structure of the signal and the noise. Examples are given of the application of the transform to images with both real and synthetic noise.

The techniques considered in this paper are based on a number of mathematical results, none of which are proved here. Proofs can be found in an unpublished report [6], which will be provided on request to the authors.

II. The Maximum Noise Fraction (MNF) Transform

We have seen (Fig. 1) that the principal components transform does not always produce images that show steadily decreasing image quality with increasing component number. The question thus arises: Can we design a linear transformation that will always perform this function? One of the most common measures of image quality is the signal-to-noise ratio. Thus, instead of choosing new components to maximize variance, as the principal components transform does, we now choose them to maximize the signal-to-noise ratio. Our choice should then achieve the desired optimal ordering in terms of image quality.

This transformation can be defined in several ways. It can be shown that the same set of eigenvectors is obtained by procedures that maximize either the signal-to-noise ratio or the noise fraction. This latter measure was used in our previous work [5] and has been retained here for com-

Manuscript received November 21, 1986; revised August 10, 1987.

A. Green and M. Craig are with the CSIRO Division of Mineral Physics and Mineralogy, P.O. Box 136, North Ryde, NSW 2113, Australia.

M. Berman is with the CSIRO Division of Mathematics and Statistics, P.O. Box 218, Lindfield, NSW 2070, Australia.

P. Switzer is with the Department of Statistics, Stanford University, Stanford, CA 94305.

IEEE Log Number 8717523.

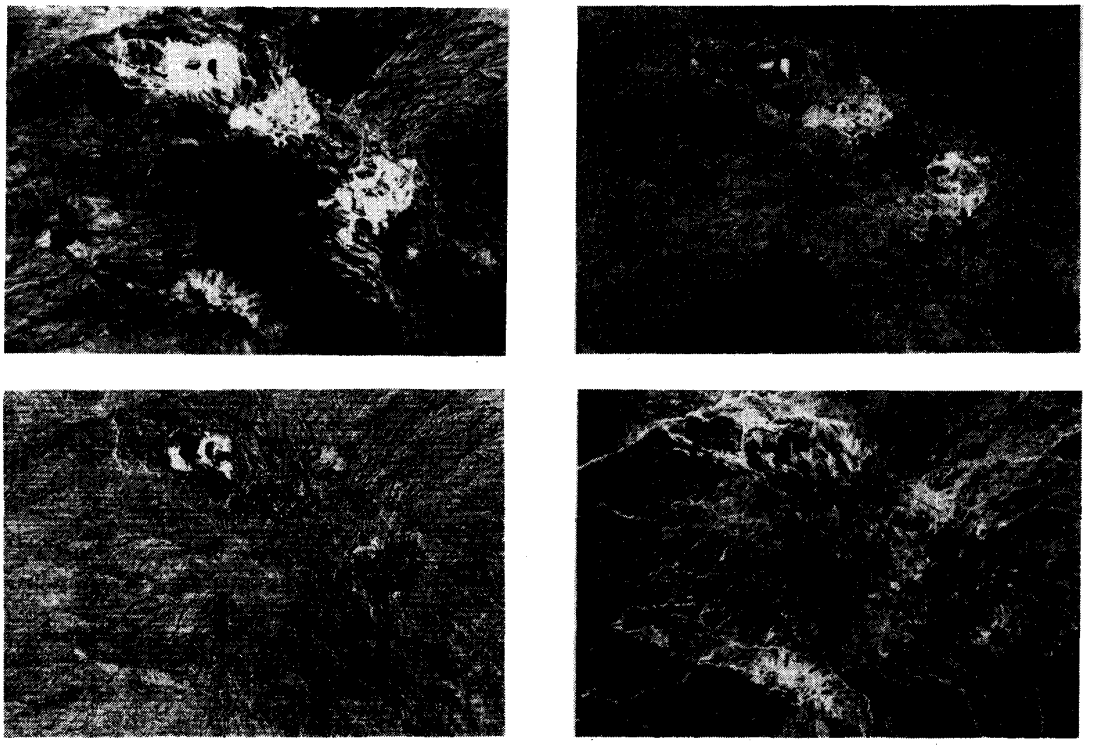

Fig. 1. First, fourth, sixth, and ninth principal component images for ten-band ATM data acquired over Silver Bell, Arizona.

patibility. We stress that all the results described can be obtained from either measure.

Let us consider a multivariate data set of p-bands with grey levels

$$Z_i(x), \qquad i = 1, \cdots, p$$

where x gives the coordinates of the sample. We shall assume that

$$\boldsymbol{Z}(x) = \boldsymbol{S}(x) + \boldsymbol{N}(x)$$

where $\boldsymbol{Z}^T(x) = \{Z_1(x), \cdots, Z_p(x)\}$, and $\boldsymbol{S}(x)$ and $\boldsymbol{N}(x)$ are the *uncorrelated* signal and noise components of $\boldsymbol{Z}(x)$. Thus

$$\text{Cov}\left\{\boldsymbol{Z}(x)\right\} = \boldsymbol{\Sigma} = \boldsymbol{\Sigma}_S + \boldsymbol{\Sigma}_N$$

where $\boldsymbol{\Sigma}_S$ and $\boldsymbol{\Sigma}_N$ are the covariance matrices of $\boldsymbol{S}(x)$ and $\boldsymbol{N}(x)$, respectively. Note that, although we are assuming additive noise, the techniques described in this paper in principle can also be applied to multiplicative noise by first taking logarithms of the observations.

We define the noise fraction of the i^{th} band to be

$$\text{Var}\left\{N_i(x)\right\}/\text{Var}\left\{Z_i(x)\right\}$$

the ratio of the noise variance to the total variance for that band. The maximum noise fraction (MNF) transform chooses linear transformations

$$Y_i(x) = \boldsymbol{a}_i^T\boldsymbol{Z}(x), \qquad i = 1, \cdots, p$$

such that the noise fraction for $Y_i(x)$ is maximum among all linear transformations orthogonal to $Y_j(x)$, $j = 1, \cdots, i$.

Using arguments similar to those used in the derivation of principal components, it can be shown that the vectors $\boldsymbol{a}_i$ are the left-hand eigenvectors of $\boldsymbol{\Sigma}_N\boldsymbol{\Sigma}^{-1}$, and that μ_i, the eigenvalue corresponding to $\boldsymbol{a}_i$, equals the noise fraction in $Y_i(x)$. Hence, from the definition of the MNF transform, we see that $\mu_1 \geq \mu_2 \geq \cdots \geq \mu_p$, and so the MNF components will show steadily *increasing* image quality (unlike the usual ordering of principal components).

Throughout the rest of the paper, it will be assumed that the eigenvectors $\boldsymbol{a}_i$ are normed so that

$$\boldsymbol{a}_i^T\boldsymbol{\Sigma}\boldsymbol{a}_i = 1, \qquad i = 1, \cdots, p.$$

This norming is for mathematical convenience only, and has no effect on the noise removal procedures discussed later. It will also be convenient at certain points to express the MNF transform in the matrix form

$$\boldsymbol{Y}(x) = \boldsymbol{A}^T\boldsymbol{Z}(x)$$

where $\boldsymbol{Y}^T(x) = (Y_1(x), \cdots, Y_p(x))$ and $\boldsymbol{A} = (\boldsymbol{a}_1, \cdots, \boldsymbol{a}_p)$.

An important property of the MNF transform (not shared by principal components) is that, because it depends on signal-to-noise *ratios*, it is invariant under scale changes to any band. Another useful property is that it orthogonalizes $\boldsymbol{S}(x)$ and $\boldsymbol{N}(x)$, as well as $\boldsymbol{Z}(x)$.

To obtain the MNF transform, we need to know both Σ and Σ_N. In many practical situations, these covariance matrices are unknown and need to be estimated. Usually, Σ is estimated using the sample covariance matrix of $Z(x)$; this approach is adopted for the examples discussed in this paper.

A method that indirectly estimates Σ_N is discussed in Section V. For the moment we ignore this estimation problem and illustrate some of the properties of the MNF transform in two familiar cases.

A. Case I: Uncorrelated Noise with Equal Variance σ_N^2 in All Bands

Here the noise is spherically distributed about the data mean. Hence the directions with maximum noise fraction must be the directions of minimum overall variance. These directions are the same as those selected by a principal components analysis. This fact can be seen algebraically, because we have

$$\Sigma_N = \sigma_N^2 I.$$

Hence, by remarks above, the matrix to be diagonalized will be $\sigma_N^2 \Sigma^{-1}$. The eigenvectors of Σ and Σ^{-1} are identical, and, as the principal components procedure diagonalizes Σ, we see that the two procedures will produce the same set of eigenvectors. The eigenvalues of Σ^{-1} are the inverses of the eigenvalues of Σ.

The equivalence of the two procedures in this special case probably explains the success of principal components analysis in ordering image quality for many remotely sensed data sets. Therefore, the noise in all bands of these data may have been approximately equal and uncorrelated across bands.

When the noise variances are known, but unequal, it is simple to rescale the data so that all bands have equal noise variance. Principal components analysis can then be used to obtain an optimal ordering of image quality.

In the even more special case where there is also perfect between-band signal correlation, the same variable is being measured p times (apart possibly from scale factors). In this situation the transformation produces new components where, in the MNF space, only the p^{th} component has any signal.

B. Case II: Noise in One Band Only

Not surprisingly, in this case the noise is best isolated by choosing a new component $Y_1(x)$ that is composed of the noisy band minus that linear combination of the noise-free bands that best estimates the signal component of the noisy band (in the sense of minimizing the variance of their difference). If a high correlation exists between the signal component of the noisy band and the noise-free bands, then a good estimate can be obtained and the resulting image will be mostly noise. Let

$$\Sigma^{-1} = (v_{ij}), \qquad 1 \le i, j \le p$$

and assume that noise is all in the first band. Then, if σ_N^2 is the noise variance in band 1, it can be shown that

$$\mu_1 = \sigma_N^2 v_{11}$$

$$\mu_i = 0, \qquad i = 2, \cdots, p$$

and

$$a_1^T = v_{11}^{-1/2}(v_{11}, v_{12}, \cdots, v_{1p}).$$

Hence, all the noise is retained in the first MNF component and the remaining MNF components are all linear combinations of the noise-free bands. It can further be shown that, if $S_i(x)$ is the signal component of band i, then the values of $\beta_2, \cdots, \beta_p$ minimizing

$$\text{Var}\left\{S_1(x) - \Sigma_2^p \beta_i S_i(x)\right\}$$

are proportional to $v_{12}, \cdots, v_{1p}$, respectively (as given in a_1^T above). It should also be noted that, in this case, it is not necessary to know σ_N^2 in order to define the MNF transform.

III. Noise Removal

Once data have been transformed into components with decreasing noise fraction (increasing S/N ratio), it is logical to spatially filter the noisiest components and subsequently to transform back to the original coordinate system. As the transformed components filtered by this procedure contain a reduced signal component, the resulting signal degradation will be much less than if the same smoothing were performed on the untransformed data. This procedure should allow much more intense smoothing to be applied without serious signal degradation.

Noise reduction is achieved by using the high between-band correlation that often exists in the signal components of remotely sensed data. A multivariate signal can be considered to lie between two extremes: perfect between-band correlation and zero between-band correlation. In the former case, we would expect to be able to achieve a maximal noise reduction (viz. var (S)/var (N) improved by a factor of p if the S/N ratio is constant). In the latter case no improvement can be made by the procedures discussed here. The amount of noise reduction achieved in each situation depends on the degree of between-band correlation, the relative powers of the noise in each input band, and the type of smoothing performed on the transformed components.

In general, although the low-order MNF components contain more noise, they still have a signal constituent. If these signals need to be retained, each MNF component must be filtered before retransformation to obtain a cleaned image. Under these conditions it is difficult to estimate the losses in both signal and noise, as they are dependent upon the nature of the filtering process. However, when the signal content of a MNF component is so low that it can be neglected, it is easy to estimate the signal and noise losses in such a process.

In the next section we investigate the consequences of a constraining process that sets the noisiest component to a constant value (namely the component mean) before transformation back to the original space. This constrain-

ing process may be considered as an ultimate smoothing operation. The generalization to the case where more than one component is constrained is straightforward, but is not discussed here.

A. The Effect of Constraining the First MNF Component

The constraining process outlined above can be considered to be premultiplication by a matrix $\boldsymbol{R}$ whose components are unity in the last $p-1$ diagonal elements and zero elsewhere. Thus, we have

$$\boldsymbol{Y}^*(x) = \boldsymbol{R}\boldsymbol{Y}(x)$$

and the vector of filtered values is

$$\boldsymbol{Z}^*(x) = (\boldsymbol{A}^{-1})^T \boldsymbol{Y}^*(x).$$

In addition, the whole process of noise removal can be condensed into a single linear transformation

$$\boldsymbol{Z}^*(x) = (\boldsymbol{A}^{-1})^T \boldsymbol{R}\boldsymbol{A}^T\boldsymbol{Z}(x).$$

For notational convenience we let $\boldsymbol{b}_1^T$ denote the first row of $\boldsymbol{A}^{-1}$.

Then it can be shown that

$$\text{Cov}\left\{\boldsymbol{Z}^*(x)\right\} = \boldsymbol{\Sigma} - \boldsymbol{b}_1\boldsymbol{b}_1^T$$

and the noise and signal components of $\boldsymbol{Z}^*(x)$ have covariance matrices

$$\text{Cov}\left\{\boldsymbol{S}^*(x)\right\} = \boldsymbol{\Sigma}_S - (1-\mu_1)\boldsymbol{b}_1\boldsymbol{b}_1^T$$

$$\text{Cov}\left\{\boldsymbol{N}^*(x)\right\} = \boldsymbol{\Sigma}_N - \mu_1\boldsymbol{b}_1\boldsymbol{b}_1^T.$$

The differences between the raw and filtered data are interesting.

We can write

$$\begin{aligned}\boldsymbol{Z}(x) - \boldsymbol{Z}^*(x) &= \boldsymbol{b}_1\boldsymbol{a}_1^T\boldsymbol{Z}(x)\\ &= \boldsymbol{b}_1 Y_1(x)\end{aligned}$$

where $Y_1(x)$ is the MNF component corresponding to the largest eigenvalue μ_1. Hence, all p difference images are scalar multiples of $Y_1(x)$. It is also interesting to consider the effects of this filtering process in the special cases noted in the previous section. In some instances, we shall use the *traces* of the covariance matrices of $S(x)$, $N(x)$, $S^*(x)$, and $N^*(x)$ as simple measures of the total variation due to signal and noise in the original and filtered processes.

When all bands have noise, with equal variances σ_N^2, which is uncorrelated across bands (Case I), let $\rho_1 \geq \rho_2 \geq , \cdots \geq \rho_p$ denote the eigenvalues of $\boldsymbol{\Sigma}$ which has trace t. It can be shown that

$$t_N^* = tr\left[\text{Cov}\left\{\boldsymbol{N}^*(x)\right\}\right] = (p-1)\sigma_N^2,$$

$$\begin{aligned}t_S^* &= tr\left[\text{Cov}\left\{\boldsymbol{S}^*(x)\right\}\right]\\ &= t - \rho_p - (p-1)\sigma_N^2.\end{aligned}$$

Then if we use $f^* = t_N^*/(t_S^* + t_N^*)$ as a measure of the noise fraction in the filtered images and let $f = p\sigma_N^2/t$ denote the analogous noise fraction in the original images, we can see that

$$f^*/f = t(p-1)/(t-\rho_p)p.$$

As ρ_p is often very small, the noise removal procedure will reduce the noise fraction by a factor of about p^{-1}.

When noise occurs in one band only (Case II), we have seen that the first MNF component contains both noise and signal, while the other MNF components are noise-free. If, as previously, the noise is in the first band, it can be shown for the constraining and inversion process that

$$\boldsymbol{b}_1^T = (v_{11}^{-1/2}, 0, 0, \cdots, 0)$$

and using this one obtains

$$\begin{aligned}\boldsymbol{Z}^*(x) = \boldsymbol{S}^*(x) = \Big[&\theta_1 - v_{11}^{-1}\sum_{i=2}^{p} v_{1i}(Z_i(x) - \theta_i),\\ &Z_2(x), \cdots, Z_p(x)\Big]^T, \quad \boldsymbol{N}^*(x) = \boldsymbol{0}\end{aligned}$$

where θ_i, $i = 1, \cdots, p$, is the mean for band i. The results above show us that all the noise in band 1 has been removed, the pure signal in bands 2 to p has been retained, and band 1 has been replaced by a linear combination of the other bands. Indeed, it follows from earlier comments that, in this case, the above MNF-constrained estimator of the signal component of band 1 is the best linear combination of the signals in bands 2 to p in a mean-squared-error sense. In fact, if $\boldsymbol{\Sigma}$ is estimated using the sample covariance matrix, this estimator can be shown to be equivalent to that obtained from ordinary least squares regression of band 1 on bands 2 to p. The signal loss in the constraining procedure above can be estimated from $tr[\text{Cov}\{\boldsymbol{S}(x) - \boldsymbol{S}^*(x)\}]$ and is found to be $v_{11}^{-1} - \sigma_N^2$.

In all the discussion thus far, we have assumed that we know $\boldsymbol{\Sigma}$ and $\boldsymbol{\Sigma}_N$. In general, this will not be so, and although the method for estimating $\boldsymbol{\Sigma}$ is apparent, the method for estimating $\boldsymbol{\Sigma}_N$ is not. In the special case where noise occurs in one band only (Case II) this does not cause a problem and this case is treated in the next section. The subsequent section then treats one possible solution to the more complex case when the noise is in more than one band.

IV. Examples of Noise Removal When Noise is in One Band Only

There are many examples of remotely sensed multispectral data where one band of a set will have considerably more noise than others that are highly correlated with it. If the spatial characteristics of the noise are such that it cannot be removed without degrading real picture detail, the procedures above can be used with great effect. The example of the Silver Bell data shown in Fig. 1 serves to illustrate this point.

The ten-band original data for this scene are composed of six relatively clean images and four that have varying types of noise.

The band 1 image is badly degraded by salt-and-pepper noise, the band 4 image has a strong periodic horizontal striping pattern, and the two shortwave infrared bands,

9(~ 1.6 μm) and 10(~ 2.2 μm), have approximately periodic striping at a low angle to the scan line direction (probably caused by microphonics).

Because the noise characteristics vary from band to band, the principal components transform provides a nonoptimal ordering of image quality. Also, because the various types of noise have such different spatial characteristics, it is very difficult to devise a procedure to estimate the overall noise covariance matrix.

We can, however, treat the noisy bands one at a time and use their correlation structure with the six other good bands, which are assumed noise free, to clean them. Fig. 2 shows the original noisy band 1 image (Fig. 2(a)) and the first MNF component (out of seven) when the analysis is applied to band 1 (Fig. 2(b)). Virtually no signal remains in the MNF image and the constraining procedure outlined in the previous section is applicable.

It is now clear that if we are prepared to throw away the residuals shown in Fig. 2(b), we are really saying that band 1 contains no information that could not be obtained from the other "noise-free" bands. This is because our reconstituted cleaned band 1 will be formed merely from a linear combination of the "noise-free" bands. Thus, unless we need to see a clean image with the reflectance characteristics of band 1, we may as well ignore it completely and proceed with our data analysis using only the "noise-free" bands.

A more realistic application of the method is to consider the noise in bands 4 and 10. (The case of band 9 is similar to that for band 10 and will not be discussed further.)

Fig. 3(a)–(b) illustrates the original band 4 image and the first MNF component. Again the noise is concentrated into the MNF band although some signal has also been included. Filtering of Fig. 3(b) and subsequent inverse transformation results in a cleaned band 4 image. In this case, because of the specific spatial pattern of the noise, a simple notch filter in the Fourier domain produces improved image quality, whether it is applied to the MNF image as described above or to the original noisy band 4 image.

There is much less correlation between the shortwave infrared (~ 2.2 μm) band 10 (Fig. 4(a)), and the noise-free bands at shorter wavelengths. As a result, the first MNF component (Fig. 4(b)) has significant signal content.

In keeping with the idea of spatially filtering the noisy MNF component before transforming back to the original coordinate system, the image in Fig. 4(b) was low-pass filtered using a symmetric Gaussian taper in the frequency domain. After application of the inverse of the MNF transformation, a cleaned band 10 image resulted. To illustrate the change made to the original band 10 image, the cleaned image was subtracted from the original. The result is shown in Fig. 5(b).

The original band 10 image was also low-pass filtered with the same filter as was applied to the MNF image. The result was also subtracted from the original to produce Fig. 5(a). Although the same low-pass filter was used

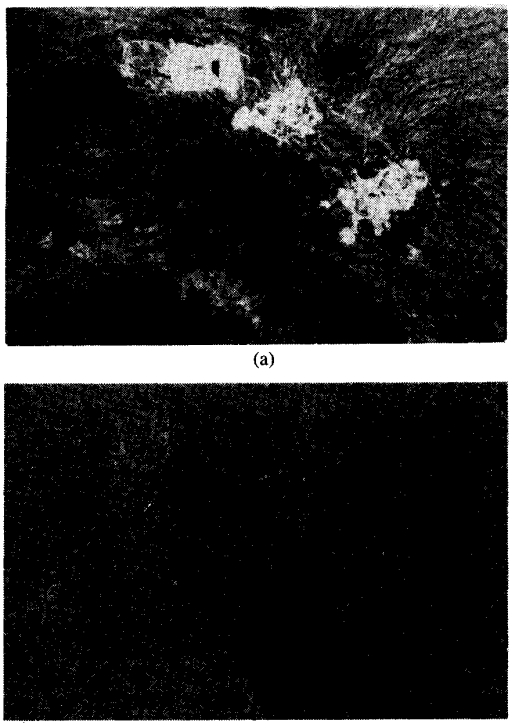

(a) (b)

Fig. 2. (a) Band 1 ATM image for the Silver Bell data. Notice the random noise pattern. (b) First MNF component computed assuming only band 1 contains noise and using the remaining six "noise free bands."

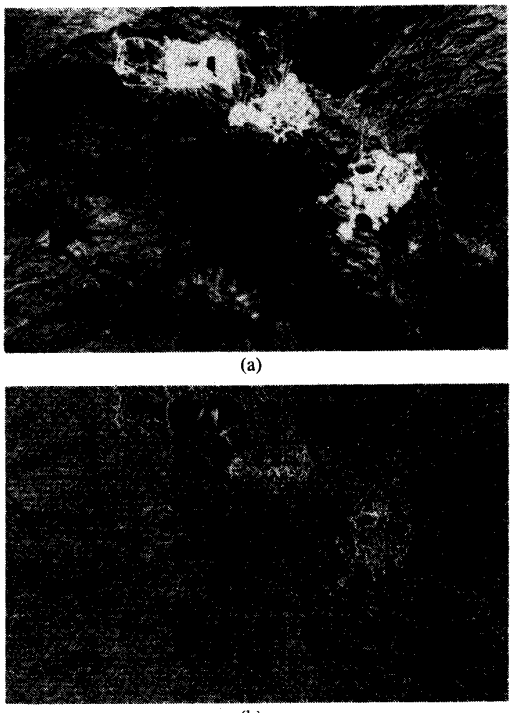

(a) (b)

Fig. 3. (a) Band 4 ATM image for the Silver Bell data. (b) First MNF component calculated assuming only band 4 contains noise and using the remaining six "noise free" bands. Some picture detail remains with a greatly enhanced noise pattern.

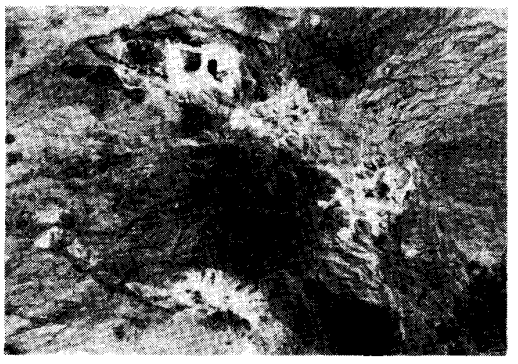

(a)

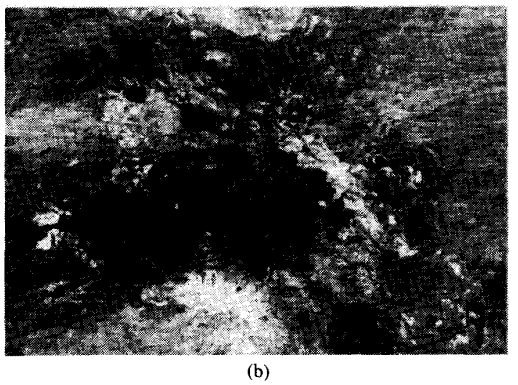

(b)

Fig. 4. (a) Band 10 shortwave infrared ATM image for the Silver Bell data. (b) First MNF component using image in 4(a) and the noise free bands as in Figs. 2 and 3.

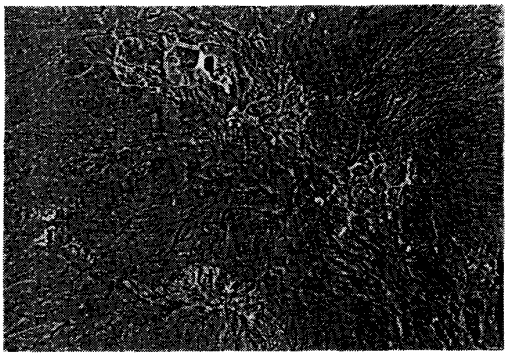

(a)

(b)

Fig. 5. (a) Image obtained by subtracting a low-pass filtered version of band 10 from the original band 10 data. The filter characteristics were chosen so as to smooth most of the noise appearing as low-angle stripping. (b) Image obtained by subtracting a cleaned version of band 10 from the original band 10 data. The cleaning was performed by applying the same low-pass filter as used to produce Fig. 5(a) to the first MNF component shown in Fig. 4(b) followed by retransformation to the original coordinate system.

in both cases, considerably more signal was removed when it was used directly than in combination with the MNF transformation. Just how much signal has been lost unnecessarily is shown in Fig. 6, which is the difference between the two images shown in Fig. 5(a) and 5(b).

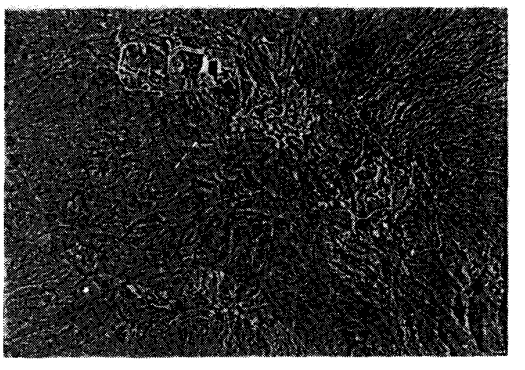

Fig. 6. Difference between Fig. 5(a) and (b). An illustration of the detail unnecessarily removed by filtering the raw data, instead of transforming to the MNF space before filtering.

V. Noise in More Than One Band

When there is noise in more than one band and its covariance structure is not known, we must find some way of estimating it from the data. In general, this will involve computing the covariance matrix of new variables resulting from some type of spatial filtering of each input band. The selection of the appropriate filter must be determined by the spatial characteristics of the noise that it is designed to isolate, and on the spatial characteristics of the signal in which it is buried. No filter will extract noise completely. Hence, careful analysis will be required to establish the conditions under which the covariance matrix so generated approximates Σ_N.

Switzer and Green [5] developed a procedure known as minimum/maximum autocorrelation factors (MAF), which in effect estimates the noise covariance matrix for certain kinds of noise. This procedure exploits the fact that, in most remotely sensed data, the signal at any point in the image is strongly correlated with the signal at neighboring pixels, while the noise shows only weak spatial correlations. It is, therefore, applicable to salt-and-pepper noise, as well as to other forms of signal degradation such as striping.

The MAF transform chooses p orthogonal linear combinations $Y_i(x) = \boldsymbol{a}_i^T \mathbf{Z}(x)$ showing increasing spatial correlation. Specifically, if Δ is a small spatial lag, then the

vectors $\boldsymbol{a}_i$ are chosen so that

$$\text{Corr}\left(Y_i(x), Y_i(x+\Delta)\right) = \text{Corr}\left(\boldsymbol{a}_i^T\mathbf{Z}(x), \boldsymbol{a}_i^T\mathbf{Z}(x+\Delta)\right)$$

is a minimum, subject to being orthogonal to previously defined components $Y_k(x)$ where $k < i$. When the noise is weakly autocorrelated compared with the signal, the low-numbered factors are mostly noise and the high-numbered factors are mostly signal. Typically, $\Delta = (1, 0)$ (a horizontal neighbor) or (0, 1) (a vertical neighbor) for salt-and-pepper noise, while $\Delta = (0, 1)$ is usually appropriate for horizontal striping noise.

This MAF transform can be formulated in terms of the covariance matrices of the data and of the between-neighbor differences. Specifically, the vectors $\boldsymbol{a}_i$ are the left-hand eigenvectors of $\boldsymbol{\Sigma}_\Delta\boldsymbol{\Sigma}^{-1}$, where $\boldsymbol{\Sigma}_\Delta = \text{Cov}\{\mathbf{Z}(x) - \mathbf{Z}(x+\Delta)\}$. At this point we note that $\boldsymbol{\Sigma}_\Delta\boldsymbol{\Sigma}^{-1}$ has the same form as $\boldsymbol{\Sigma}_N\boldsymbol{\Sigma}^{-1}$, and that $\boldsymbol{\Sigma}_\Delta$ is to some extent a measure of the noise, as it contains little of the covariance structure of the strongly autocorrelated signal.

How well does $\boldsymbol{\Sigma}_\Delta$ measure the covariance structure of the noise ($\boldsymbol{\Sigma}_N$)? Switzer and Green [5] considered a simple proportional covariance model that can provide some answers to this question. This model assumes:

1) Signal $S(x)$ and noise $N(x)$ are uncorrelated, with
2) $\text{Cov}\{S(x), S(x+\Delta)\} = b_\Delta\boldsymbol{\Sigma}_S$
   $\text{Cov}\{N(x), N(x+\Delta)\} = c_\Delta\boldsymbol{\Sigma}_N$

where b_Δ and c_Δ are constants when between-neighbor correlations are considered and b_Δ is much larger than c_Δ. Perhaps the most important consequence of the proportional covariance model is that the signal (and noise) correlation at lag Δ is the same in all bands, namely b_Δ (and c_Δ). Under this model it can be shown that

$$1/2\,\boldsymbol{\Sigma}_\Delta = (1 - b_\Delta)\boldsymbol{\Sigma} + (b_\Delta - c_\Delta)\boldsymbol{\Sigma}_N.$$

If the signal has high spatial autocorrelation, $\text{Cov}\{S(x), S(x+\Delta)\}$ will be very similar to $\boldsymbol{\Sigma}_S$, i.e., $b_\Delta \sim 1$. Also for salt-and-pepper noise $\text{Cov}\{N(x), N(x+\Delta)\}$ will be approximately zero, implying $c_\Delta \sim 0$. Under these circumstances we have $\boldsymbol{\Sigma}_N \sim 1/2\,\boldsymbol{\Sigma}_\Delta$. However, even when b_Δ and c_Δ do not approach the limits above, the following results can be obtained under proportional covariance.

1) The eigenvectors of $\boldsymbol{\Sigma}_\Delta\boldsymbol{\Sigma}^{-1}$ are the same as those of $\boldsymbol{\Sigma}_N\boldsymbol{\Sigma}^{-1}$ and are thus independent of b_Δ and c_Δ. In addition, the noise fraction in each new component is independent of b_Δ and c_Δ.

2) The eigenvectors of $\boldsymbol{\Sigma}_\Delta\boldsymbol{\Sigma}^{-1}(\lambda_i)$, and $\boldsymbol{\Sigma}_N\boldsymbol{\Sigma}^{-1}(\mu_i)$ are related by

$$\mu_i = \frac{\lambda_i/2 - (1 - b_\Delta)}{b_\Delta - c_\Delta}.$$

3) Because $0 \le \mu_i \le 1$ it follows that

$$c_\Delta \le 1 - \lambda_i/2 \le b_\Delta \quad \text{for all } i.$$

Hence, by considering the largest λ_i we can obtain an upper bound for c_Δ, and by considering the smallest λ_i we can obtain a lower bound for b_Δ. When $b_\Delta \sim 1$ and $c_\Delta \sim 0$, $\lambda_i/2$ becomes an approximate estimator for the proportion of $\text{Var}\{Y_i(x)\}$ that is due to noise. However, it also has an exact interpretation. It is easily shown that

$$1 - \lambda_i/2 = \text{corr}\left\{Y_i(x), Y_i(x+\Delta)\right\}$$

(i.e., $1 - \lambda_i/2$ is the correlation between neighboring pixels in the i^{th} MAF component).

(a)

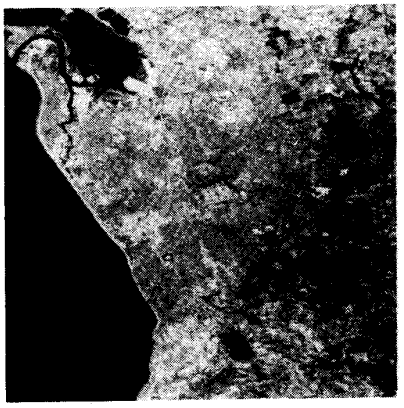

(b)

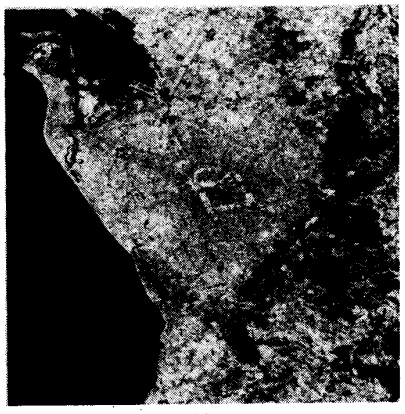

(c)

Fig. 7. Landsat MSS images of Adelaide, South Australia with noise added to bands 4(a), 5(b), and 6(c). The added noise has zero mean and variances 20 (band 4), 5 (band 5), and 10 (band 6).

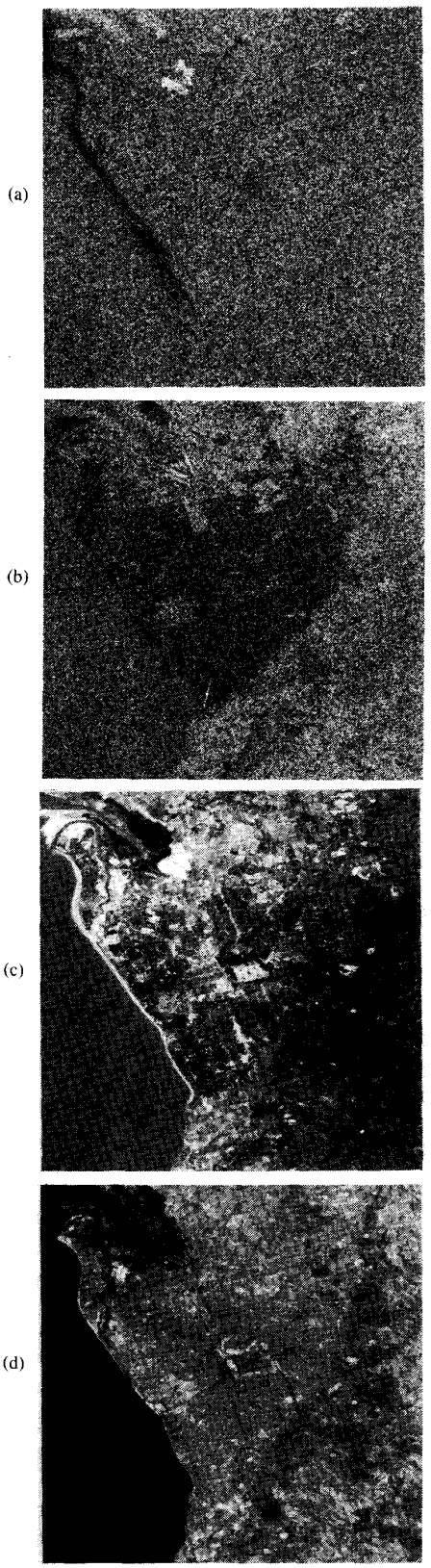

Fig. 8. MAF images corresponding to the images in Fig. 7. Almost all the picture information is concentrated into the last two MAF components.

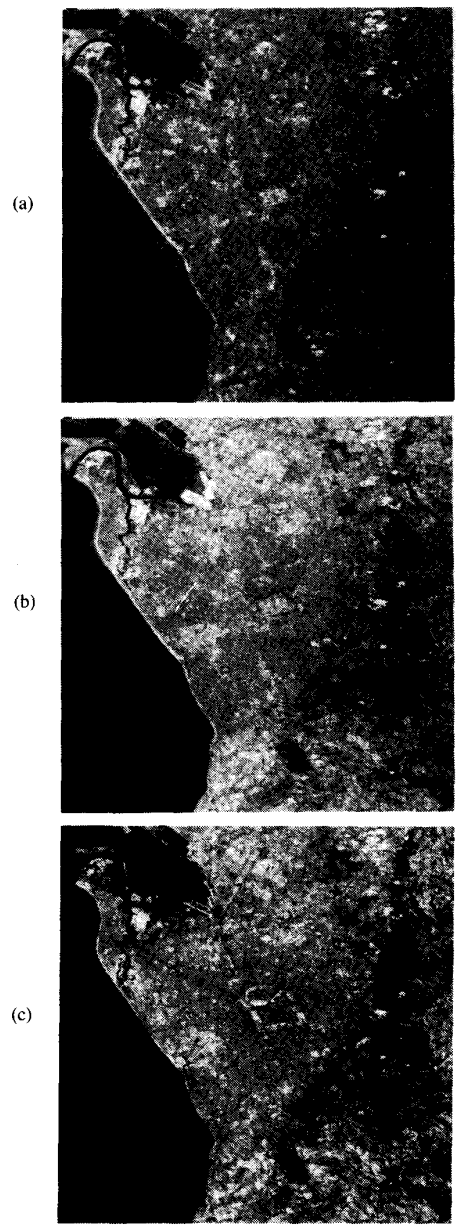

Fig. 9. Cleaned images corresponding to Fig. 7. These images were obtained by smoothing the images shown in Fig. 8(a) and (b), and retransformation back to the original MSS coordinate system.

We have carried out some preliminary analyses into the validity of the proportional covariance model, and into methods for estimating b_Δ and c_Δ. It would appear that the model provides a reasonable approximation to reality for many remotely sensed images. We hope to publish detailed results after further analyses.

VI. Noise Removal by MAF

As the MAF procedure uses between-neighbor differences to estimate the noise covariances, it is particularly useful for isolating salt-and-pepper noise. If the procedure is applied to the Silver Bell data discussed above, it

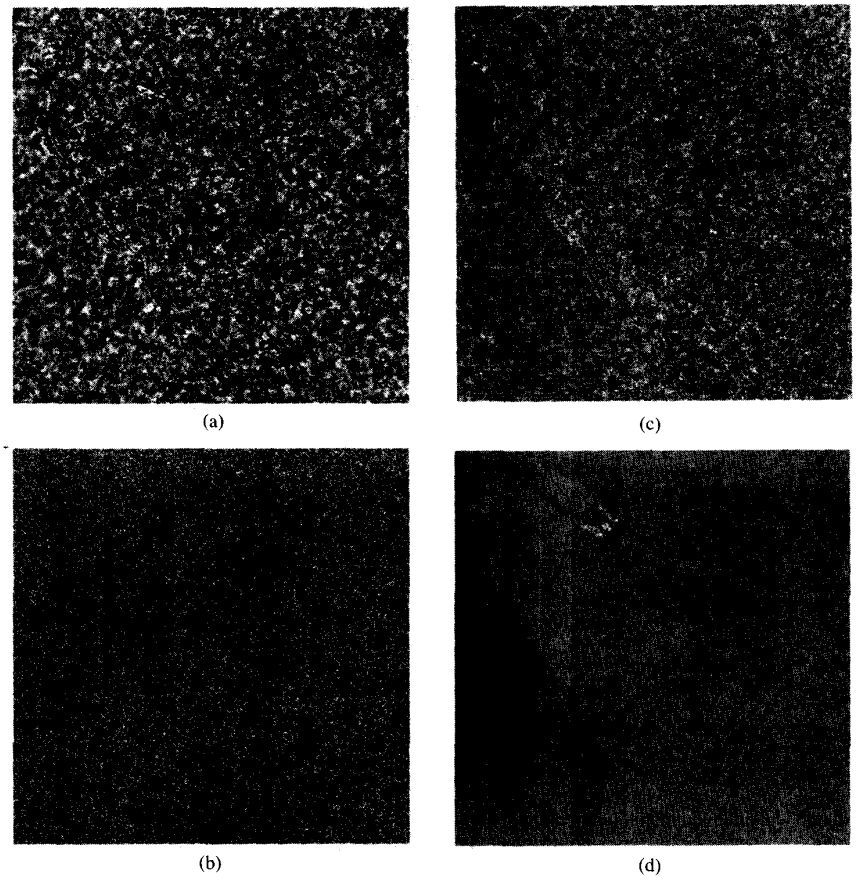

Fig. 10. Difference images between those shown in Fig. 9 and the raw MSS data *before* noise was added. Only a small amount of image detail has not been recovered by the cleaning procedure. (a) Cleaned—original band 4, (b) cleaned—original band 5, (c) cleaned—original band 6, (d) cleaned—original band 7.

effectively extracts the noise in band 1 (which is of this type), but it does not isolate the low-angle striping in bands 9 and 10. This behavior is to be expected as there is no single lag Δ that will allow the estimation of a Σ_N encompassing the three different types of noise present in the data. For this reason we applied the MNF transform to the noisy Silver Bell bands one at a time in Section IV.

Having no simple examples where salt-and-pepper noise is strong in more than one band, we have created a synthetic example using a segment of a Landsat MSS image over Adelaide in South Australia. Fig. 7 shows the results of adding spatially uncorrelated Gaussian noise with no band-to-band correlations, zero means, and standard deviations of 20, 5, and 10 to bands 4, 5, and 6, respectively. No noise was added to band 7. Principal components images of these data did not provide a good separation of the signal and noise. However, it can be seen that the first two MAF images (Fig. 8(a) and (b)) show almost no image signal information. These two images were low-pass filtered with a symmetrical Gaussian taper in the frequency domain and the MAF transformation was inverted to produce the cleaned images shown in Fig. 9. There is a dramatic improvement in the image quality over that shown in Fig. 7. Fig. 10 shows the difference images between the cleaned images of Fig. 9 and the original Landsat data *before* noise was added. These differences show that only a small amount of image detail has not been recovered by the cleaning procedure.

VII. Conclusions

The MNF transform discussed in this paper has the ability to provide an optimal ordering of images in terms of image quality. It is identical with the standard principal components transformation when the noise variances in all bands are equal and is equivalent to a form of multiple linear regression when noise is in one band only.

As the low order MNF components have a greatly increased noise fraction, intense filtering procedures can be applied to them without serious degradation to the signal content of the data. Subsequent retransformation results in cleaned images with little signal loss.

When noise occurs in one band only, it is not necessary to estimate the noise covariance matrix. However, in more complicated cases this matrix must be estimated. The

MAF procedure discussed here provides one method of doing so for salt-and-pepper noise, and the conditions under which its results estimate Σ_N have been determined.

The high between-band correlation that often exists in remotely sensed multispectral scanner data means that these systems are in some sense making multiple measurements of the same quantity. The extent of this redundancy is, of course, reflected in the magnitudes of the eigenvalues of the signal covariance matrices. In situations when these matrices have only a few significant eigenvalues the techniques discussed here will provide a powerful tool for noise reduction.

References

[1] A. Singh and A. Harrison, "Standardized principal components," *Int. J. Remote Sensing*, vol. 6, pp. 883-896, 1985.

[2] P. J. Ready and P. A. Wintz, "Information extraction, SNR improvement, and data compression in multispectral imagery," *IEEE Trans. Commun.*, vol. 21, pp. 1123-1130, 1973.

[3] A. R. Gillespie, "Digital techniques of image enhancement," in *Remote Sensing in Geology*, B. S. Siegal and A. R. Gillespie, Eds. New York: Wiley, 1980, pp. 195-202 and pp. 220-203.

[4] J. R. G. Townshend, "Agriculture land-cover discrimination using thematic mapper spectral bands," *Int. J. Remote Sensing*, vol. 5, no. 4, pp. 681-698, 1984.

[5] P. Switzer and A. Green, "Min/max autocorrelation factors for multivariate spatial imagery," Dept. of Statistics, Stanford University, Tech. Rep. 6, 1984.

[6] M. Berman, "The statistical properties of three noise removal procedures for multichannel remotely sensed data," CSIRO Division of Mathematics and Statistics Consulting Rep., NSW/85/31/MB9, 1985.

*

Andrew A. Green received the B.Sc. and Ph.D. degrees in physical chemistry from the University of Western Australia.

After two years of post-doctoral work at the Department of Applied Earth Sciences at Stanford University, he joined the CSIRO Division of Mineral Physics and is now Assistant Chief of the Division. He has worked on developing remote-sensing techniques for mineral exploration, including studies of the spectral reflectance properties of rocks and soils and the development of image-processing techniques for the enhancement of Landsat data.

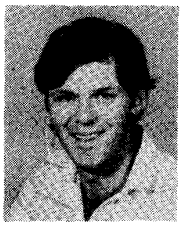

Mark Berman received the B.Sc.(Hons.) degree and University Medal in mathematical statistics from the University of New South Wales in 1974, and the Master of Statistics degree from the same institution in 1976. In 1978, he was awarded the Ph.D. and D.I.C. degrees in mathematical statistics by the Imperial College of Science and Technology, London.

He was a visiting lecturer in the Department of Statistics at the University of California, Berkeley during 1978-1979, and since 1979 he has been with the CSIRO Division of Mathematics and Statistics, Sydney, where he is now a Senior Research Scientist. He regularly consults and collaborates with members of the CSIRO Divisions of Mineral Physics and Mineralogy, and Applied Physics. His recent research interests have mainly been in statistical methods for spatial processes, especially remote sensing, image processing, and spatial point processes.

*

Paul Switzer received the B.S.(Hons.) degree in mathematics from the University of Manitoba, Canada, in 1961, and the A.M. and Ph.D. degrees in statistics from Harvard University, Cambridge, MA, in 1963 and 1965, respectively.

Since 1965 he has held a joint appointment in the Department of Statistics and the School of Earth Sciences at Stanford University, Palo Alto, CA, where he is now Professor. He is currently Editor of the Journal of the American Statistical Association, and Vice President of the International Association for Mathematical Geology. His recent research interests include the development and application of statistical methods to problems in remote sensing, image processing, and environmental science.

*

Maurice D. Craig received the B.Sc. degree in 1965 and the M.Sc. degree in 1968 from the University of Sydney and the Ph.D. degree in 1972 from the University of Michigan, Ann Arbor.

Following teaching appointments in mathematics at the University of Toronto, the State University of New York, Buffalo, and Western Illinois University, Macomb, IL, he joined the CSIRO Division of Mineral Physics in 1981 and has been involved with the processing of remotely sensed data for mineral exploration.